

Separation of quadrupolar and magnetic contributions to spin–lattice relaxation in the case of a single isotope

A. Suter, M. Mali, J. Roos, and D. Brinkmann

Physik-Institut, Universität Zürich, CH-8057 Zürich, Switzerland

We present a NMR pulse double-irradiation method which allows one to separate magnetic from quadrupolar contributions in the spin–lattice relaxation. The pulse sequence fully saturates one transition while another is observed. In the presence of a $|\Delta m| = 2$ quadrupolar contribution, the intensity of the observed line is altered compared to a standard spin–echo experiment. We calculated analytically this intensity change for spins $I = 1, 3/2, 5/2$, thus providing a quantitative analysis of the experimental results. Since the pulse sequence we used takes care of the absorbed radio-frequency power, no problems due to heating arise. The method is especially suited when only *one* NMR sensitive isotope is available. Different cross-checks were performed to prove the reliability of the obtained results. The applicability of this method is demonstrated by a study of the plane oxygen ^{17}O ($I = 5/2$) in the high-temperature superconductor $\text{YBa}_2\text{Cu}_4\text{O}_8$: the ^{17}O spin–lattice relaxation rate consists of magnetic as well as quadrupolar contributions.

PACS numbers:

I. INTRODUCTION

The work presented in this paper has been motivated by the experience in condensed matter nuclear magnetic resonance (NMR) experiments that quite often both magnetic and quadrupolar time dependent interactions are present causing spin–lattice relaxation. The question arises whether it is possible to deduce, directly from the experiment, the admixture of the two different contributions to the overall relaxation.

The literature contains mainly calculations of multiexponential magnetization recovery laws for the case of either *purely* magnetic or *purely* quadrupolar fluctuations, with Andrew *et al.*¹ being the first to treat the case of a static quadrupolar perturbed Zeeman Hamiltonian (spin $I = 3/2, 5/2$). These calculations were extended to higher spins^{2–4} and to the case of a static quadrupolar Hamiltonian^{5–8}. MacLaughlin *et al.*⁹ treated the case of a static quadrupolar Hamiltonian ($\eta = 0$) with mixed fluctuations in a kind of perturbation expansion, whereas Rega¹⁰ presented, for this case, an exact solution in the limit of time approaching zero.

In a previous study¹¹, we discussed the multiexponential recovery for the case of a static quadrupolar perturbed Zeeman Hamiltonian in the presence of both magnetic and quadrupolar fluctuations under the assumption that the spin–exchange coupling can be omitted and the eigenfunctions of the static Hamiltonian can be approximated by Zeeman eigenfunctions. We found that, in a surprisingly large region of the parameter space spread by the probabilities for magnetic and quadrupolar induced transitions, it is almost impossible, within experimental errors, to separate magnetic and quadrupolar contributions to the relaxation. Instead, the “dominant” contribution determines the time evolution of the recovery law, *i.e.* the system can approximately be described by a *single* time constant, T_1^{eff} . However, it is questionable whether this approximation is meaningful in the presence of mixed relaxation or whether it is more appropriate to

describe the system by the *separate* transition probabilities.

If the nucleus under consideration has *two* magnetic isotopes as in the case of copper (^{63}Cu and ^{65}Cu), the admixture can be estimated from the ratio of the relaxation times, T_1 . Nevertheless, the precision needed for a reliable interpretation of this ratio is commonly underestimated.

In this publication we will present a method, which enables the experimentalist to separate the different contributions of the spin–lattice relaxation especially in the case where the element under consideration has only *one* NMR sensitive isotope. The method involves a special initial condition of the spin system which we call dynamic saturation and which had already been mentioned briefly in our previous work¹¹.

The paper is organized as follows. The next section will introduce the theoretical background essential to understand the method. In Sec. III we will give the results including a discussion, and Sec. IV will show experimental results of ^{17}O NMR in $\text{YBa}_2\text{Cu}_4\text{O}_8$ including a more technical discussion of the experiment.

II. BASIC RELATIONS AND MASTER EQUATION

For simplicity and the reader’s convenience, we repeat part of our treatment presented in Ref. ¹¹. The starting point is the following Hamiltonian:

$$\mathcal{H}_{\text{tot}} = \mathcal{H}_0 + \mathcal{H}_1(t),$$

where $\mathcal{H}_0 = \mathcal{H}_Z + \mathcal{H}_Q$ describes the time-independent (or “static”) Hamiltonian which comprises the Zeeman interaction, \mathcal{H}_Z , with the external magnetic field and the quadrupolar interaction, \mathcal{H}_Q , with the internal electric field gradient (EFG) tensor. $\mathcal{H}_1(t)$ takes into account fluctuations; it is the sum of a magnetic and a quadrupolar contribution:

$$\mathcal{H}_1(t) = \mathcal{H}_{\text{mag}}(t) + \mathcal{H}_{\text{quad}}(t), \quad (1)$$

where

$$\begin{aligned} \mathcal{H}_{\text{mag}}(t) &= -\hbar\gamma_n \mathbf{I} \cdot \mathbf{h}(t) \\ \mathcal{H}_{\text{quad}}(t) &= \frac{eQ}{4I(2I-1)} \sum_{k=-2}^2 V_k(t) T_{2k}(\mathbf{I}). \end{aligned}$$

Here, \mathbf{I} is the nuclear spin operator, $\mathbf{h}(t)$ is a fluctuating magnetic field, $V_k(t)$ is a component of the fluctuating EFG, and $T_{2k}(\mathbf{I})$ are spherical tensor operators^{12,13}.

In Eq. (1), nuclear spin–exchange terms were omitted. If the quadrupolar splitting, due to \mathcal{H}_Q , is large compared to the nuclear spin–exchange coupling, the time evolution of the spin–lattice relaxation proceeds by the direct coupling to the lattice. Cases where the nuclear spin–exchange terms are important are discussed in Refs.^{1,14}.

The relaxation of the spin system towards its thermodynamic equilibrium is described by the so–called master equation

$$\frac{d}{dt} \mathbf{P}(t) = \mathbf{W} \{ \mathbf{P}(t) - \mathbf{P}(0) \}. \quad (2)$$

Here, $\mathbf{P}(t)$ is the population vector of the different energy levels with $\mathbf{P}(0)$ being the equilibrium value. The relaxation matrix, \mathbf{W} , is, in second order perturbation theory, given by¹²

$$\begin{aligned} W_{\alpha\beta} \quad \alpha \neq \beta &\stackrel{\text{def}}{=} \frac{1}{\hbar^2} \int_{-\infty}^{\infty} d\tau \exp(i\omega_{\alpha\beta}\tau) \overline{\langle \alpha | \mathcal{H}_1(\tau) | \beta \rangle \langle \beta | \mathcal{H}_1(0) | \alpha \rangle} \\ W_{\alpha\alpha} &= - \sum_{\beta \neq \alpha} W_{\alpha\beta}, \end{aligned}$$

where $|\alpha\rangle$, $|\beta\rangle$ are eigenstates of \mathcal{H}_0 and $\omega_{\alpha\beta} = (\langle \alpha | \mathcal{H}_0 | \alpha \rangle - \langle \beta | \mathcal{H}_0 | \beta \rangle) / \hbar$ are transition frequencies. Ensemble averages are denoted by $\overline{\langle \dots \rangle}$.

As long as the eigenfunctions of \mathcal{H}_0 can be approximated by the eigenfunctions of a Zeeman Hamiltonian, *i.e.* $\|\mathcal{H}_Z\| \gg \|\mathcal{H}_Q\|$, the relevant relaxation matrix terms for magnetic and quadrupolar relaxation are given as follows:

$$\begin{aligned} W_{\alpha\beta}^{\text{mag}} &= J(\omega_{\alpha\beta}) \cdot \{ |\langle \alpha | I^+ | \beta \rangle|^2 + |\langle \alpha | I^- | \beta \rangle|^2 \} \\ W_{\alpha\beta}^{\text{quad},1} &= J^{(1)}(\omega_{\alpha\beta}) \cdot \{ |\langle \alpha | I^+ I_z + I_z I^+ | \beta \rangle|^2 + \\ &\quad + |\langle \alpha | I^- I_z + I_z I^- | \beta \rangle|^2 \} \\ W_{\alpha\beta}^{\text{quad},2} &= J^{(2)}(\omega_{\alpha\beta}) \cdot \{ |\langle \alpha | (I^+)^2 | \beta \rangle|^2 + \\ &\quad + |\langle \alpha | (I^-)^2 | \beta \rangle|^2 \}. \end{aligned}$$

The J 's are the spectral densities of the fluctuating fields:

$$\begin{aligned} J(\omega) &= \frac{\gamma_n^2}{2} \int_{-\infty}^{\infty} d\tau \exp(i\omega\tau) [h_+, h_-] \\ J^{(1,2)}(\omega) &= \left(\frac{eQ}{\hbar} \right)^2 \int_{-\infty}^{\infty} d\tau \exp(i\omega\tau) [V_{+1,2}, V_{-1,2}] \end{aligned}$$

with $[A, B] = (1/2) \overline{(A(\tau)B(0) + B(\tau)A(0))}$, $h_{\pm} = h_x \pm ih_y$, $V_{\pm 1} = V_{xz} \pm iV_{yz}$, and $V_{\pm 2} = \frac{1}{2}(V_{xx} - V_{yy}) \pm iV_{xy}$.

If \mathcal{H}_Z and \mathcal{H}_Q are of similar magnitude, the situation is more complicated. The case of *purely magnetic fluctuations*, for $\|\mathcal{H}_Z\| \approx \|\mathcal{H}_Q\|$, has been treated by various authors^{15,16}.

In this paper, we will deal with the case $\|\mathcal{H}_Z\| \gg \|\mathcal{H}_Q\|$ and we make the additional assumption that the spectral densities can be approximated by a single value. This means that the inverse of the correlation time, τ_c^{-1} , of the fluctuating fields is large compared to $\omega_{\alpha\beta}$, that is $\omega_{\alpha\beta}\tau_c \ll 1$. One then obtains:

$$\begin{aligned} J(\omega) &\simeq J(0) =: W \\ J^{(1,2)}(\omega) &\simeq J^{(1,2)}(0) =: W_{1,2} \end{aligned}$$

and the resulting transition probabilities become

$$\begin{aligned} W_{m \rightarrow m-1}^{\text{mag}} &= W (I+m)(I-m+1) \\ W_{m \rightarrow m-1}^{\text{quad},1} &= W_1 \frac{(2m-1)^2 (I-m+1)(I+m)}{2I(2I-1)^2} \\ W_{m \rightarrow m-2}^{\text{quad},2} &= W_2 \frac{(I+m)(I+m-1)(I-m+1)(I-m+2)}{2I(2I-1)^2}. \end{aligned}$$

Our calculations were performed in the high–temperature limit, *i.e.* $\hbar\omega_{\alpha\beta} \ll k_B T$, so that a further simplification takes place: $W_{\alpha \rightarrow \beta} \simeq W_{\beta \rightarrow \alpha}$. Fig. 1 sketches the various transition probabilities which are possible for a 5/2 spin system. We assume the spacings between the levels to be sufficiently unequal to suppress spin–exchange transitions.

To solve the master equation, Eq. (2), it is convenient to introduce some abbreviations. The population of level m is P_m and we define the difference in population between adjacent levels by $P_{m+1/2} = P_{m+1} - P_m$; the equilibrium value of this difference is $n_0 = P_{m+1}(0) - P_m(0)$. The deviation of the population difference from its equilibrium value is denoted by $N_{m+1/2} = P_{m+1/2} - n_0$; the values $N_{m+1/2}$ form the vector \mathbf{N} .

Given the transition probabilities as shown in Fig. 1, we can write down, in compact form, the following “reduced” master equation for \mathbf{N} :

$$\frac{d}{dt} \mathbf{N} = \mathbf{R} \mathbf{N}, \quad (3)$$

where \mathbf{R} is the reduced relaxation coefficient matrix. The solution of Eq. (3) is of the form

$$N_j(t) = \sum_i \left[(\mathbf{E}^T)^{-1} \mathbf{N}(0) \right]_i E_{ij} \exp(t\lambda_i), \quad (4)$$

where λ_i and \mathbf{E} are the eigenvalues and the eigenvector matrix of \mathbf{R} , respectively, and \mathbf{E}^T denotes the transposed of \mathbf{E} . $\mathbf{N}(0)$ is the vector describing the initial condition of the spin system into which it has been brought during a certain preparation period.

Once the $N_j(t)$ are known, the corresponding time dependent magnetization, $M(t)$, is obtained:

$$M(t) = M(\infty) \left[1 - \sum_i a_i \exp(t\lambda_i) \right] \quad (5)$$

and the a_i are given by

$$a_i = -\frac{1}{n_0} \left[(\mathbf{E}^T)^{-1} \mathbf{N}(0) \right]_j E_{ji}, \quad (6)$$

where the index j refers to the line which will be observed, *e.g.* the central transition. Usually, the irradiated line and the observed line are the same.

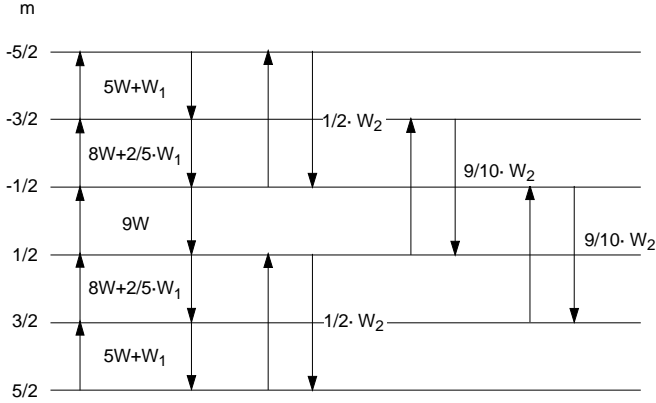


FIG. 1. Transitions between the spin energy levels effected by magnetic and quadrupolar spin-lattice relaxation processes for $I = 5/2$.

We will now consider an experiment, which we call *dynamic saturation*, with a special initial condition; this pulse sequence will allow us to disentangle quadrupolar from magnetic contributions in the spin-lattice relaxation. We saturate a selected line, q , for instance by a long comb of pulses in such a way that the comb length, T_{tot} , is much larger than $1/\min(W, W_1, W_2)$ and that the pulse spacing, T_{CD} , within the comb satisfies the condition $5T_2 < T_{\text{CD}} \ll 1/\max(W, W_1, W_2)$. This situation contrasts with an adiabatic manipulation of the spin system where, with the spin system initially in equilibrium, a short radio-frequency (RF) pulse is applied to one of the transitions. In the case of dynamic saturation, the initial condition must be calculated since the stimulating RF field causes transitions, with transition rate P_{rf} , between the levels $q+1/2$ and $q-1/2$. Thus, for calculating the initial condition vector, the rate equation (3) must be extended in the following way:

$$\frac{d}{dt} \mathbf{N} = (\mathbf{R} + \mathbf{S}) \mathbf{N} + n_0 \mathbf{P}.$$

\mathbf{S} is a square matrix with all elements zero except $S_{q\pm 1, q} = P_{\text{rf}}$, $S_{q, q} = -2P_{\text{rf}}$. \mathbf{P} is a vector with all the elements zero except $P_{q\pm 1} = P_{\text{rf}}$, $P_q = -2P_{\text{rf}}$. For dynamic equilibrium, when $d\mathbf{N}/dt = 0$, we have

$$\mathbf{N}(\infty) = -n_0 (\mathbf{R} + \mathbf{S})^{-1} \mathbf{P}.$$

$\mathbf{N}(\infty)$, which becomes the initial condition vector $\mathbf{N}(0)$ for solving Eq. (3), is calculated under the assumption

that $P_{\text{rf}} \gg \max(W, W_1, W_2)$. The exact formulas for $\mathbf{N}(0)/n_0$ are given in Appendix A.

III. TRANSITION ENHANCEMENT BY DYNAMIC SATURATION

Let us deal, for the moment, with the special situation of *pure* magnetic relaxation, *i.e.* $W_1, W_2 = 0$. In this case, after dynamic saturation, the $\mathbf{N}(0)$'s for all spin values $I \geq 1$ take the form

$$\mathbf{N}(0)/n_0 = [0, \dots, 0, -1, 0, \dots, 0]$$

where -1 refers to the irradiated line. This equation reflects the following behavior. On the time scale of the spin-lattice relaxation, $T_1 = 1/(2W)$, the new population differences are the same as in the case of thermodynamic equilibrium, except for the irradiated line. That means that a spectrum obtained by adiabatic manipulation (*e.g.* in a standard spin-echo experiment) is identical with the corresponding spectrum due to dynamic saturation, except for the irradiated line. This is not true anymore in the case of mixed or pure quadrupolar relaxation as we will show now.

The intensity of a specific transition which we observe will be denoted as follows. $I_{\text{ad}}|_{m \rightarrow m-1}$ is measured by an adiabatic pulse sequence as in the case of a standard $\pi/2 - \pi$ spin echo experiment; $I_{\text{dyn}}|_{m \rightarrow m-1}^{n \rightarrow n-1}$ refers to the same transition, $m \rightarrow m-1$, however, in the presence of dynamic saturation of the transition $n \rightarrow n-1$. Given this notation, we define an *enhancement factor* by

$$E_{m \rightarrow m-1}^{n \rightarrow n-1} = \frac{I_{\text{dyn}}|_{m \rightarrow m-1}^{n \rightarrow n-1}}{I_{\text{ad}}|_{m \rightarrow m-1}} = 1 + \left(\frac{\mathbf{N}(0)}{n_0} \right)_{m-1/2}$$

With the results of Appendix A we get, for instance, for a spin $I = 5/2$ system with the central transition being dynamically saturated and the inner satellite being observed: $E_{\pm 3/2 \rightarrow \pm 1/2}^{1/2 \rightarrow -1/2} = 1 + \mu_5/\zeta_1$. The enhancement factor is *one* in the case of pure magnetic relaxation but it is nontrivial in the case of mixed or pure quadrupolar relaxation.

That the enhancement factor is a nontrivial function of the relaxation process was already noticed by Pound¹⁷ who used it to show that ^{23}Na ($I = 3/2$, 100% abundance) in NaNO_3 relaxes purely quadrupolar.

Fig. 2 shows, for a spin $I = 5/2$ system with mixed relaxation, contour plots of the enhancement factor as a function of W_1/W and W_2/W . Similar results, however less pronounced, are found for other combinations of $n \rightarrow n-1$ and $m \rightarrow m-1$.

The characteristic results are as follows. (i) The enhancement effect is less pronounced in the case of mixed relaxation as compared to pure quadrupolar relaxation. This makes it more difficult to detect the effect, although not impossible because of the very high time stability of modern spectrometers. (ii) There is always at least one

transition with an appreciable enhancement factor [e.g. the cases (a) and (c) in Fig. 2], whereas the other transitions are “depressed” [cases (b) and (d)]. This feature can be used for crosschecking the experiment if one is able to observe both transitions at the same time; this will be demonstrated in the next section. (iii) The enhancement factor depends only weakly on W_1/W since W_1 connects, except for the $(-1/2, 1/2)$ -transition, the same levels as W does, which has no effect on the enhancement function. Therefore, measuring the enhancement yields information only about the quadrupolar $\Delta m = 2$ transitions.

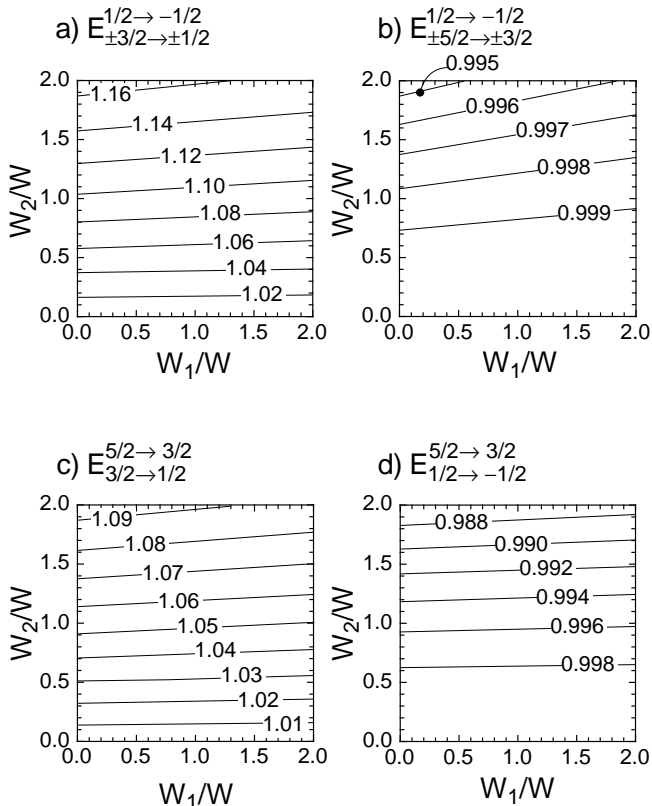


FIG. 2. Contour plots of the enhancement for a spin $I = 5/2$ system in the case of mixed relaxation. (a) and (b) correspond to saturation of the central transition, (c) and (d) to saturation of the outer high-frequency satellite.

IV. EXPERIMENTAL DETAILS

We will discuss experimental details guided by our study of the high-temperature superconductor $\text{YBa}_2\text{Cu}_4\text{O}_8$; these investigations will be published elsewhere¹⁸.

The experiment was performed by using a combination of two standard pulse spectrometers together with a magnetic field of $B_0 = 8.9945$ T, ($B_0 \parallel c$). The resonant circuit was damped by a 12Ω resistor in order to achieve a broad frequency range. The resonance signals were obtained by a phase alternating add-subtract spin-echo technique similar to that one described in Ref. 19

followed by Fourier transformation of the spin-echo.

Each experiment consists of a certain combination of pulse sequences which are shown in Fig. 3. To measure I_{dyn} , we apply the *saturation* and the *detection* sequence. In the first sequence, dynamic saturation of the $n \rightarrow n-1$ transition is achieved by applying pulses C and D . The spacing between these pulses, T_{CD} , has to be much larger than T_2 and much shorter than T_1 , i.e. $5T_2 < T_{CD} \ll T_1$. The length of these pulses is chosen very large ($20 \mu\text{s}$) in order to saturate the $n \rightarrow n-1$ transition only. Furthermore, we change the phase between the C and D pulses by 90° to get rid of possible coherence effects. The total length of the saturation sequence, T_S , has to be of the order of the longest effective relaxation time. The *detection* sequence is the usual spin-echo $\pi/2 - \pi$ pulse sequence. Here, we use very intense pulses (the $\pi/2$ pulse length is about $1 \mu\text{s}$) to observe both the central transition and the high-frequency satellites in a single shot.

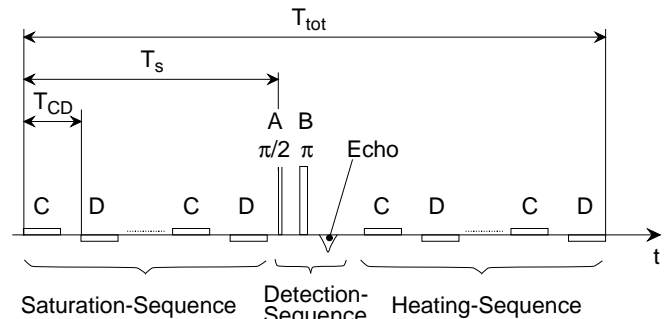


FIG. 3. Pulse sequence used in the experiment. Details are described in the text.

In order to measure I_{ad} , we apply, of course, the detection sequence, but it must be supplemented by a *heating* sequence. Since pulsing heats the sample, a comparison of line intensities of different experiments (standard spin-echo and dynamic saturation) requires constant sample temperature. This is achieved by making the heating and the saturation sequence identical so that the total power absorbed by the sample is the same in either case. In other words, the total length of the pulse sequence, T_{tot} , is kept fixed ($T_{\text{tot}} = 400$ ms in our case). From our previous experiments on the isotope effect of the spin gap²⁰ we know that, at about 95 K, a constant temperature is achieved after running the heating sequence for about 5 minutes. A combination of all three pulse sequences is used to cross-check our results; this will be discussed further below.

To illustrate the method, we present ^{17}O spectra from $\text{YBa}_2\text{Cu}_4\text{O}_8$ taken at $T = 95$ K, see Fig. 4. This superconductor contains, beside the apex oxygen, plane oxygen sites, O(2) and O(3), in the CuO_2 plane, where superconductivity takes place, and a chain oxygen site, O(1). Here, we are only interested in the plane sites. Fig. 4 a) shows the ^{17}O spectrum as obtained by Fourier transform of the standard echo. All central transitions coincide, all O(1) satellites nearly coincide, while inner and

outer O(2,3) satellites are well separated. The splitting of these satellites is due to the orthorhombic symmetry ($a = 3.8411 \text{ \AA}$, $b = 3.8718 \text{ \AA}$) of the crystal.

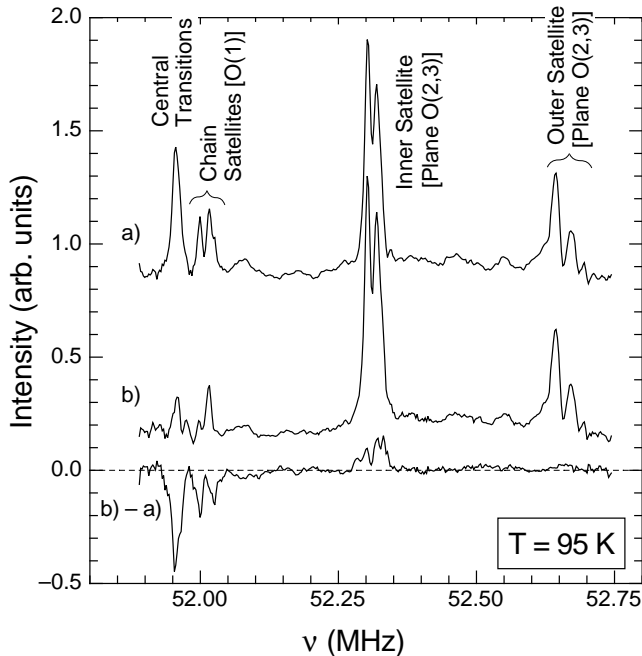


FIG. 4. a) ^{17}O central transitions and high-frequency satellites of plane oxygen, O(2) and O(3), and chain oxygen sites, O(1), in $\text{YBa}_2\text{Cu}_4\text{O}_8$. b) Spectrum obtained after dynamic saturation of the central transition. Bottom: Difference of b) and a) spectrum.

Fig. 4 b) presents the ^{17}O spectrum after dynamic saturation of the central transition and Fig. 4 c) gives the difference between the “saturation” and the “standard”. Because of the short A and B pulses, all transitions can be observed. Obviously, the central transition is saturated, note the “negative” intensity. Whereas the central transition of the plane oxygen is totally saturated, the central transition as well as the satellites of chain oxygen are not. This is due to the fact that the chain oxygen nuclei have a considerably shorter T_1 than the plane nuclei and that the pulse sequence was optimized for plane oxygen. That this is true could be proven by the symmetric experiment where we dynamically saturated the outer high-frequency satellite.

The most important feature is the remaining *positive* intensity of the difference spectrum at the position of the inner high-frequency satellite. According to the discussion above and, in particular, the contour plot of Fig. 2 (a), this intensity enhancement clearly shows that there is a quadrupolar contribution to the relaxation of the plane oxygen nuclei. This conclusion is supported by the fact that the intensity at the position of the *outer* high-frequency satellite is almost zero in agreement with the contour plot of Fig. 2 (b).

The amount of quadrupolar admixture to the overall spin-lattice relaxation is determined as follows. Experi-

mentally, the intensity enhancement of the inner satellite (when the central transition is dynamically saturated) is 1.13(2) which then results in a ratio $W_2/W = 1.4(3)$ according to Fig. 2 (a). If we saturate the *outer* high-frequency satellite, the intensity enhancement of the inner satellite is 1.04(2), leading to a ratio of $W_2/W = 0.7(4)$ according to Fig. 2 (c). The weighted average is: $W_2/W = 1.15(25)$.

It is more difficult to determine the ratio W_1/W since the enhancement factor $E_{\pm 3/2 \rightarrow \pm 1/2}^{1/2 \rightarrow -1/2}$ depends only weakly on W_1 . However, we can estimate this ratio indirectly, to be shown below; we found that $W_1 \leq W/3$.

To cross-check the results, we also performed an experiment with the so-called *gradual saturation sequence* which involves the application of all three pulse sequences as they are shown in Fig. 3. T_s is the duration of the saturation sequence. By I_s we denote the intensity of a line in case of gradual saturation while I_0 is the intensity of the line in the standard spin-echo sequence (including the heating sequence). The *gradual intensity enhancement* is then defined as I_s/I_0 . In Fig. 5, we have plotted this enhancement for the central transition (top figure) and for the outer satellite (bottom) as a function of T_s . Bullets refer to inner satellites (top and bottom), open circles to outer satellites (top), and triangles (bottom) to the central transition.

For short T_s , the inner satellites (denoted by bullets) are strongly enhanced as expected, since in the case of an ideal $\pi/2$ -pulse (adiabatic manipulation) at the central transition or outer satellite, respectively, I_s/I_0 should reach the value 1.5. Due to spin-lattice relaxation processes this value decays towards a limit which is (for T_s reaching a value corresponding to dynamical saturation) one in the case of pure magnetic relaxation and different from one in the case of mixed or pure quadrupolar relaxation.

The response of the outer satellite and the central transition enhancement is retarded, since spin-lattice relaxation processes need some time for “pumping” these transitions. This explains the enhancement maximum around $T_s = 40 \text{ ms}$, before the enhancement starts to diminish towards one in the limit of dynamic saturation ($T_s \simeq 300 \dots 350 \text{ ms}$). In this limit, that is for $T_s \rightarrow 1/\min(W, W_1, W_2)$, we have, according to Sec. III and Fig. 2, $I_s/I_0 \rightarrow E_{m \rightarrow m-1}^{1/2 \rightarrow -1/2}$. This is the result discussed above.

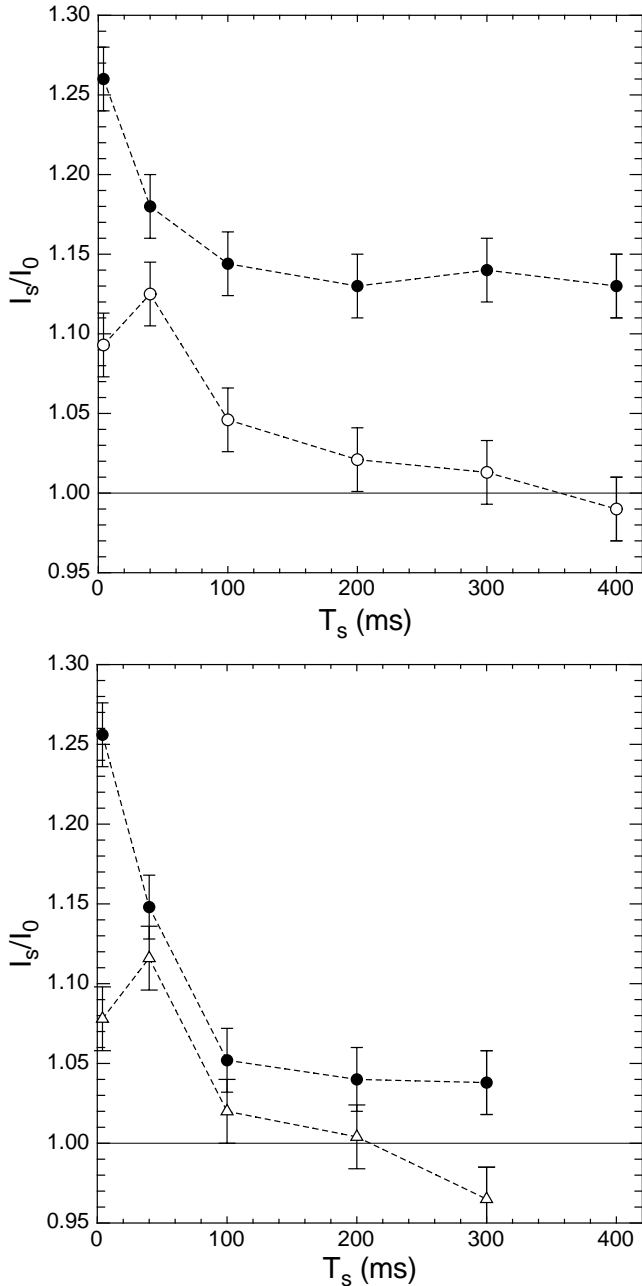


FIG. 5. Top: Gradual saturation of central transition. Bullets (open symbols) represent the intensity enhancement of the inner (outer) high-frequency satellites. Bottom: Gradual saturation of outer high-frequency satellite. Bullets (triangles) represent the intensity enhancement of the inner high-frequency satellite (central transition).

We are now able to estimate the ratio W_1/W . I_s/I_0 of the inner satellite decays very fast within the first 100 ms which corresponds to $T_1^{\text{eff}} = 101(5)$ ms at $T = 95$ K which we had measured previously²¹ by the standard inversion recovery method. However, dynamical saturation is achieved only at around 300...350 ms. Therefore, a slow relaxation rate must be involved. Because $W_2/W \approx 1$, we conclude that this slow relaxation rate has to be W_1 , i.e. $W_1 \leq W/3$. This clearly shows that the spin-lattice

relaxation process contains a strong quadrupolar contribution which could not be detected otherwise so far. The discussion of the origin of this effect, which does not arise from phonons, as well as its temperature dependence will be given elsewhere¹⁸.

V. SUMMARY

We have presented a pulse double-irradiation method which allows one to separate magnetic from quadrupolar contributions in the spin-lattice relaxation. The pulse sequence fully saturates one transition while another is observed. The clue is that the observed transition changes its intensity if and only if a $|\Delta m| = 2$ quadrupolar contribution is present; the change is monitored with respect to a standard spin-echo experiment. We calculated analytically this intensity change for spins $I = 1, 3/2, 5/2$, thus providing a quantitative analysis of the experimental results. Since the presented pulse sequence takes care of the absorbed radio-frequency power, no problems due to heating arise. The method is especially suited when only *one* NMR sensitive isotope is available. Different cross-checks were performed to prove the reliability of the obtained results.

The applicability of the method is demonstrated by a study of the plane oxygen ^{17}O ($I = 5/2$) in the high-temperature superconductor $\text{YBa}_2\text{Cu}_4\text{O}_8$. We showed that the spin-lattice relaxation rate consists of magnetic as well as quadrupolar contributions.

ACKNOWLEDGMENTS

The partial support of this work by the Swiss National Science Foundation is gratefully acknowledged.

APPENDIX A: ANALYTICAL FORMULAE FOR INITIAL CONDITION VECTOR

1. Spin $I=1$

$$\frac{\mathbf{N}(0)}{n_0} = \left[\frac{\mu}{\zeta}, -1 \right], \quad \mu = 2W_2, \quad \zeta = 2W + W_1 + 2W_2$$

2. Spin $I=3/2$

(a) *Dynamic saturation of the central transition:*

$$\frac{\mathbf{N}(0)}{n_0} = \left[\frac{\mu}{\zeta}, -1, \frac{\mu}{\zeta} \right], \quad \mu = W_2, \quad \zeta = 3W + W_1 + W_2$$

(b) *Dynamic saturation of the satellite:*

$$\begin{aligned} \frac{\mathbf{N}(0)}{n_0} &= \left[-1, \frac{\mu_1}{\zeta}, \frac{\mu_2}{\zeta}\right], \\ \mu_1 &= W_2(3W + W_1 + W_2) \\ \mu_2 &= -W_2^2 \\ \zeta &= 12W^2 + 4WW_1 + 10WW_2 + 2W_1W_2 + W_2^2 \\ &+ 1056WW_1^2W_2 + \frac{64}{5}W_1^3W_2 + 16240W^2W_2^2 + \\ &+ 2744WW_1W_2^2 + \frac{336}{5}W_1^2W_2^2 + 980WW_2^3 + \\ &+ \frac{392}{5}W_1W_2^3 + 9W_2^4. \end{aligned}$$

3. Spin I=5/2

(a) *Dynamic saturation of the central transition:*

$$\begin{aligned} \frac{\mathbf{N}(0)}{n_0} &= \left[\frac{\mu_4}{\zeta_1}, \frac{\mu_5}{\zeta_1}, -1, \frac{\mu_5}{\zeta_1}, \frac{\mu_4}{\zeta_1}\right] \\ \mu_4 &= -9W_2^2 \\ \mu_5 &= 45W_2(10W + 2W_1 + W_2) \\ \zeta_1 &= 4000W^2 + 1000WW_1 + 40W_1^2 + 1100WW_2 + \\ &+ 160W_1W_2 + 45W_2^2. \end{aligned}$$

(b) *Dynamic saturation of the inner satellite:*

$$\begin{aligned} \frac{\mathbf{N}(0)}{n_0} &= \left[\frac{\mu_6}{\zeta_2}, -1, \frac{\mu_6}{\zeta_2}, \frac{\mu_7}{\zeta_2}, \frac{\mu_8}{\zeta_2}\right] \\ \mu_6 &= W_2(8000W^3 + 2000W^2W_1 + 80WW_1^2 + \\ &+ 3800W^2W_2 + 720WW_1W_2 + 16W_1^2W_2 + \\ &+ 440WW_2^2 + 46W_1W_2^2 + 9W_2^3) \\ \mu_7 &= -9W_2^2(10W + 2W_1 + W_2)^2 \\ \mu_8 &= 9W_2^3(10W + 2W_1 + W_2) \\ \zeta_2 &= 80000W^4 + 36000W^3W_1 + 4800W^2W_1^2 + \\ &+ 160WW_1^3 + 8200W^2W_2^2 + 46000W^3W_2 + \\ &+ 16800W^2W_1W_2 + 1680WW_1^2W_2 + 32W_1^3W_2 + \\ &+ 2060WW_1W_2^2 + 108W_1^2W_2^2 + 530WW_2^3 + \\ &+ 64W_1W_2^3 + 9W_2^4. \end{aligned}$$

(c) *Dynamic saturation of the outer satellite:*

$$\begin{aligned} \frac{\mathbf{N}(0)}{n_0} &= \left[-1, \frac{\mu_9}{\zeta_3}, \frac{\mu_{10}}{\zeta_3}, \frac{\mu_{11}}{\zeta_3}, \frac{\mu_{12}}{\zeta_3}\right] \\ \mu_9 &= W_2(8000W^3 + 2000W^2W_1 + 80WW_1^2 + \\ &+ 3800W^2W_2 + 720WW_1W_2 + 16W_1^2W_2 + \\ &+ 440WW_2^2 + 46W_1W_2^2 + 9W_2^3) \\ \mu_{10} &= -W_2^2(800W^2 + 200WW_1 + 8W_1^2 + \\ &+ 220WW_2 + 32W_1W_2 + 9W_2^2) \\ \mu_{11} &= 9W_2^3(10W + 2W_1 + W_2) \\ \mu_{12} &= -9W_2^4 \\ \zeta_3 &= 128000W^4 + 38400W^3W_1 + 2880W^2W_1^2 + \\ &+ 64WW_1^3 + 83200W^3W_2 + 20160W^2W_1W_2 + \end{aligned}$$

-
- ¹ E.R. Andrew and D.P. Tunstall, Proc. Phys. Soc. **78**, 1 (1961).
 - ² D.P. Tewari and G.S. Verma, Phys. Rev. **129**, 1975 (1963).
 - ³ A. Narath, Phys. Rev. **162**, 320 (1967).
 - ⁴ M.I. Gordon and M.J.R. Hoch, J. Phys. C: Solid State Phys. **11**, 783 (1978).
 - ⁵ A.C. Daniel and W.G. Moulton, J. Chem. Phys. **41**, 1833 (1964).
 - ⁶ N.E. Ainsbinder and I.G. Shaposhnikov, *Advances in Nuclear Quadrupole Resonance* (J.A.S. Smith, London, Heyden & Son Ltd., 1978).
 - ⁷ J. Chepin and Jr. J.H. Ross, J. Phys.: Condens. Matter **3**, 8103 (1991).
 - ⁸ I. Watanabe, J. Phys. Soc. Jpn **63**, 1560 (1994).
 - ⁹ D.E. MacLaughlin, J.D. Williamson, and J. Butterworth, Phys. Rev. B **4**, 60 (1971).
 - ¹⁰ T. Rega, J. Phys.: Condens. Matter **3**, 1871 (1991).
 - ¹¹ A. Suter, M. Mali, J. Roos, and D. Brinkmann, J. Phys.: Condens. Matter **10**, 5977 (1998).
 - ¹² A. Abragam, *The Principles of Nuclear Magnetism* (Clarendon, Oxford, 1961).
 - ¹³ C.P. Slichter, *Principles of Magnetic Resonance* (Springer-Verlag, New York, Berlin, Heidelberg, 1992).
 - ¹⁴ D. Brinkmann, M. Mali, J. Roos, R. Messer, and H. Birli, Phys. Rev. B **26**, 4810 (1982).
 - ¹⁵ M. Takigawa, J.L. Smith, and W.L. Hults, Phys. Rev. B **44**, 7764 (1991).
 - ¹⁶ M. Horvatić, J. Phys.: Condens. Matter **4**, 5811 (1992).
 - ¹⁷ R.V. Pound, Phys. Rev. **79**, 685 (1950).
 - ¹⁸ A. Suter, M. Mali, J. Roos, and D. Brinkmann, submitted to Phys. Rev. Lett.
 - ¹⁹ H. Zimmermann, Ph.D. thesis, Universität Zürich, 1991.
 - ²⁰ F. Raffa, T. Ohno, M. Mali, J. Roos, D. Brinkmann, K. Conder, and M. Eremin, Phys. Rev. Lett. **81**, 5912 (1998).
 - ²¹ A. Suter, M. Mali, J. Roos, D. Brinkmann, J. Karpinski, and E. Kaldis, Phys. Rev. B **56**, 5542 (1997).